

The photochemistry of Pluto's atmosphere as illuminated by New Horizons



Michael L. Wong^{a,*}, Siteng Fan^a, Peter Gao^a, Mao-Chang Liang^b, Run-Lie Shia^a, Yuk L. Yung^a, Joshua A. Kammer^c, Michael E. Summers^d, G. Randall Gladstone^{e,f}, Leslie A. Young^c, Catherine B. Olkin^c, Kimberly Ennico^g, Harold A. Weaver^h, S. Alan Stern^c,
The New Horizons Science Team

^aDivision of Geological and Planetary Sciences, California Institute of Technology, Pasadena, CA 91125 USA

^bResearch Center for Environmental Changes, Academia Sinica, Taipei 115, Taiwan

^cSouthwest Research Institute, Boulder, CO 80302, USA

^dGeorge Mason University, Fairfax, VA 22030, USA

^eSouthwest Research Institute, San Antonio, TX 78238, USA

^fUniversity of Texas at San Antonio, San Antonio, TX 78249, USA

^gNational Aeronautics and Space Administration, Ames Research Center, Space Science Division, Moffett Field, CA 94035, USA

^hThe Johns Hopkins University Applied Physics Laboratory, Laurel, MD 20723, USA

ARTICLE INFO

Article history:

Received 16 May 2016

Revised 27 August 2016

Accepted 17 September 2016

Available online 29 September 2016

Keywords:

Pluto, atmosphere

Atmospheres, composition

Atmospheres, chemistry

Photochemistry

ABSTRACT

New Horizons has granted us an unprecedented glimpse at the structure and composition of Pluto's atmosphere, which is comprised mostly of N₂ with trace amounts of CH₄, CO, and the photochemical products thereof. Through photochemistry, higher-order hydrocarbons are generated, coagulating into aerosols and resulting in global haze layers. Here we present a state-of-the-art photochemical model for Pluto's atmosphere to explain the abundance profiles of CH₄, C₂H₂, C₂H₄, and C₂H₆, the total column density of HCN, and to predict the abundance profiles of oxygen-bearing species. The CH₄ profile can be best matched by taking a constant-with-altitude eddy diffusion coefficient K_{zz} profile of $1 \times 10^3 \text{ cm}^2 \text{ s}^{-1}$ and a fixed CH₄ surface mixing ratio of 4×10^{-3} . Condensation is key to fitting the C₂ hydrocarbon profiles. We find that C₂H₄ must have a much lower saturation vapor pressure than predicted by extrapolations of laboratory measurements to Pluto temperatures. We also find best-fit values for the sticking coefficients of C₂H₂, C₂H₄, C₂H₆, and HCN. The top three precipitating species are C₂H₂, C₂H₄, and C₂H₆, with precipitation rates of 179, 95, and $62 \text{ g cm}^{-2} \text{ s}^{-1}$, respectively.

© 2016 Elsevier Inc. All rights reserved.

1. Introduction

In July 2015, New Horizons performed its historic flyby of Pluto, giving humanity an unprecedented view of the dwarf planet's atmosphere. One of New Horizons' goals was to determine the structure, composition, and variability of Pluto's atmosphere. The Alice instrument measured the full disk spectral flux in ultraviolet wavelengths between 52 and 187 nm as the Sun slid behind Pluto (ingress) and emerged on the other side (egress), about one hour after closest approach. This observation has been used to determine the temperature and vertical density profiles of N₂, CH₄, and various minor species in Pluto's atmosphere. Nearly simultaneous Earth ingress and egress occultations, observed in

the X-band uplink, provided profiles of temperature and pressure in Pluto's lower atmosphere (Gladstone et al., 2016).

Thanks to New Horizons, Pluto's basic atmospheric composition—at least at the time of the encounter—is now known. The task now falls to the modelers to explain Pluto's atmosphere, which defied expectations on multiple accounts. For instance, Pluto's atmosphere is far colder than anticipated. It has been suggested that this is due to radiative cooling by HCN (Gladstone et al., 2016). Despite its colder nature, Pluto seems to still produce photochemical hydrocarbons and nitriles—whose abundance profiles have been measured—to a significant degree. The most striking product of this photochemical factory is the extensive haze layers that New Horizons confirmed via optical images (Gladstone et al., 2016). A companion paper in this issue (Gao et al., 2016) investigates the microphysics behind haze production on Pluto.

The central goal of this study is to reproduce New Horizons' observations of CH₄, the C₂ hydrocarbons, as well as to predict

* Corresponding author.

E-mail address: mlwong@caltech.edu (M.L. Wong).

the abundances of other trace species that have not yet been detected with as much precision. The New Horizons data gives reliable measurements for CH₄ above 200 km and C₂ hydrocarbons between 800 and 200 km. Above 800 km, the signal-to-noise is too small to retrieve trace species' abundances. Below ~200 km, the measurements are no longer sensitive to CH₄, because all the photons shortward of 140 nm are gone, and this causes an artifact in the retrieval algorithm that makes the C₂H₆ detection nonphysical and the C₂H₂ detection untrustworthy. However, thanks to its strong, unique spectral features, C₂H₄ abundances are robust from 800 km to the surface.

2. Photochemical model

We use the one-dimensional Caltech/JPL chemistry-transport model KINETICS (Allen et al., 1981; Yung and DeMore, 1999) to explore the nature of Pluto's atmosphere. Because Pluto's atmospheric extent surpasses its solid body radius ($r_0 = 1187$ km), the atmosphere must be considered spherical (Krasnopolsky and Cruikshank, 1999). The model contains 40 levels ranging from the surface to ~1300 km. Our calculations incorporate 88 chemical species and over 1600 reactions (Li et al., 2015; Yung et al., 1984). We simulate the production and loss rates of trace compounds such as hydrocarbons and nitriles at each altitude, as well as their diffusive flux between altitude grids, by solving the 1-D continuity equation for a spherical atmosphere:

$$\frac{\partial n_i}{\partial t} + \frac{1}{r^2} \frac{\partial (r^2 \phi_i)}{\partial r} = P_i - L_i, \quad (1)$$

where n_i is the number density for species i , ϕ_i the vertical flux, P_i the chemical production rate, and L_i the chemical loss rate, all evaluated at time t and radius $r = r_0 + z$ (where z is the altitude above the surface). The vertical flux is given by

$$\begin{aligned} \phi_i &= -\frac{\partial n_i}{\partial r} (D_i + K_{zz}) - n_i \left(\frac{D_i}{H_i} + \frac{K_{zz}}{H_{atm}} \right) \\ &\quad - n_i \frac{\partial T}{\partial r} \left[\frac{(1 + \alpha_i) D_i + K_{zz}}{T} \right], \end{aligned} \quad (2)$$

where D_i is the species's molecular diffusion coefficient, H_i the species's scale height, H_{atm} the atmospheric scale height, α_i the thermal diffusion parameter, K_{zz} the vertical eddy diffusion coefficient, and T the temperature (Yung and DeMore, 1999).

The starting ingredients for a photochemical model are the pressure and temperature profiles of the atmosphere. For this study, we use the state-of-the-art profiles retrieved from radio occultation data recorded by New Horizons (Gladstone et al., 2016). These are presented as temperature and total density in Fig. 1.

Photochemistry is primarily driven by radiation from the Sun. However, the contribution from solar Lyman- α scattered from H atoms in the local interstellar medium is known to be significant in the outer Solar System (see, e.g., Moses et al., 1992). We adopt an enhancement factor of 1.43 based on the observations of Gladstone et al. (2015) for our photochemical model. We expect the production rates of hydrocarbons to scale with this factor, as the primary consequence of the destruction of CH₄ is the production of hydrocarbons, followed by their condensation.

CH₄ and N₂ are processed by far-ultraviolet and extreme-ultraviolet radiation, respectively, into higher-order hydrocarbons and nitriles. These photochemical products can themselves become photolyzed and interact with each other to form even more massive species. Many of these reactions are familiar and well understood, as the atmospheric chemistry of Pluto greatly resembles that of Titan (see, e.g., Wong et al., 2015).

However, photochemistry alone cannot explain trace species' overall abundances or the structure of their vertical profiles. It is clear that condensation plays an important role on Pluto.

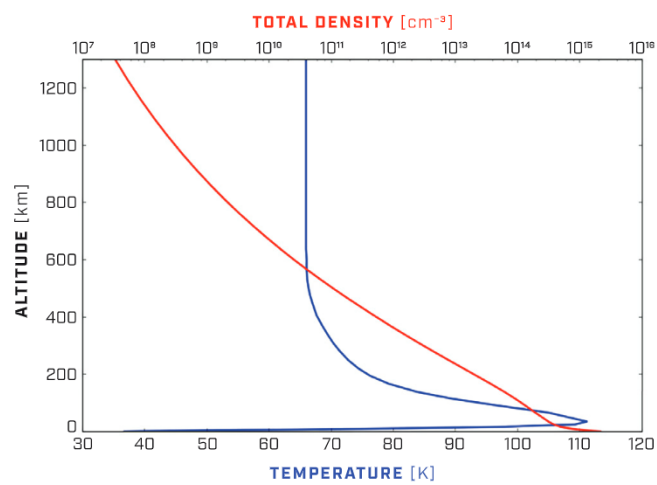


Fig. 1. The temperature and density profiles of Pluto's atmosphere, as determined by data from New Horizons.

In the New Horizons data, the major C₂ hydrocarbons increase in abundance towards the surface, but that increase is curtailed somewhere between 400 and 200 km. In a photochemical model that ignores condensation, all C₂ hydrocarbons will increase in abundance all the way to the surface, in contradiction to the data.

Saturation vapor pressures, extrapolated from laboratory measurements to Pluto temperatures, were used as a first guess to predict the condensation of various chemical species (Lara et al., 1996) (Fig. 2a). Pre-formed aerosols would serve as condensation sites. The rate coefficient J for a condensable species to be removed by collision with aerosols is given by the formalism of Willacy et al. (2016),

$$J = \frac{1}{4} \gamma v A N, \quad (3)$$

where γ is the sticking coefficient (the fraction of collisions that result in a molecule condensing upon the surface of an aerosol), v is the thermal velocity (cm s⁻¹) of the molecule, A is the surface area of an aerosol particle (cm²), and N is the number density of aerosol particles (cm⁻³). Based on a combination of observations and modeling, Gao et al. (this issue) estimate AN , the mean aerosol surface area per unit volume of atmosphere (Fig. 2b). A priori, J is highly uncertain, and we test a large range of γ to explore its impact on the condensable species.

Influx of exogenous material and escape from the top of the atmosphere are the final processes that can influence the abundances of chemical species. We incorporate a downward flux of water molecules taken from Poppe (2015), which calculated the influx of interplanetary dust into Pluto's atmosphere as a function of Pluto's location in its orbit within the Kuiper Belt. New Horizons' arrival coincides with a dust flux of 1.4×10^{-17} g cm⁻² s⁻¹. For simplicity we assume that this entire mass is composed of water ice and is vaporized within Pluto's atmosphere upon infall, thereby giving a downward H₂O flux at the top of the atmosphere of $\sim 5 \times 10^5$ molecules cm⁻² s⁻¹. In terms of loss to space, we assume all species besides H and H₂ are gravitationally bound to Pluto; we allow H and H₂ to escape at their respective Jeans escape velocities.

3. Results

3.1. CH₄

The first dataset we seek to fit is the methane abundance profile. CH₄ is the second most abundant constituent of Pluto's atmosphere and is resupplied by a large solid reservoir on the

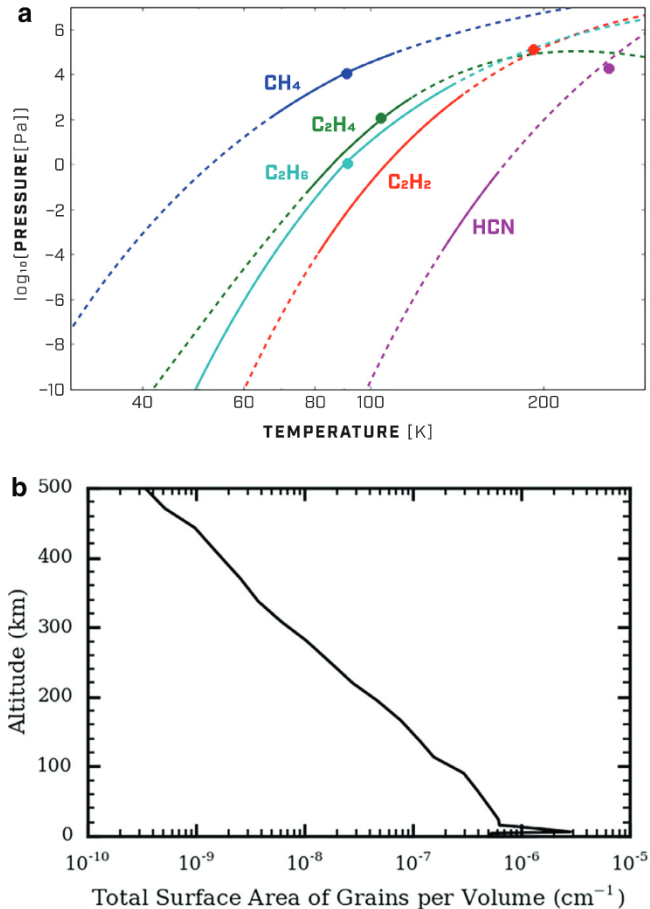


Fig. 2. (a) Saturation vapor pressure curves for various constituents of Pluto's atmosphere. Solid lines represent laboratory measurements. Dashed lines represent extrapolations. Circles indicate the triple points. (b) Total surface area of aerosols per volume of atmosphere, as calculated in our companion paper (Gao et al., 2016).

surface. Direct photolysis is the main mechanism for its loss. As the parent molecule of photochemistry, CH_4 is largely unaffected by the abundances of higher-order hydrocarbons, which we refine later (Section 3.2). Because CH_4 has a relatively long chemical lifetime, it is sensitive to transport processes. Hence, the CH_4 profile gives us information about the vertical eddy diffusion in Pluto's atmosphere.

To fit the CH_4 profile, we vary two parameters: 1) the K_{zz} profile; 2) the CH_4 mixing ratio at the surface, which we held constant during model runs. Because an analytical expression for the eddy diffusion profile of a tenuous atmosphere like Pluto's has yet to be formulated from first principles, we test a wide range of K_{zz} profiles by varying the parameter a between 0 and 1.8 in the following simple equation:

$$K_{zz} = 1000 \left(\frac{n_0}{n} \right)^a, \quad (4)$$

where n is the total number density and n_0 is the total number density at the surface. We varied CH_4 surface mixing ratios between 1×10^{-3} and 8×10^{-3} .

Changing the K_{zz} profile essentially changes the curvature of the methane profile to which the model converges. High values of a , which correspond to K_{zz} profiles that increase rapidly with altitude, produce flatter CH_4 profiles, because the methane in the upper atmosphere is being transported downwards. On the other hand, when $a = 0$, the K_{zz} profile is constant with altitude, and more CH_4 can exist in the upper atmosphere. To first order, chang-

ing the CH_4 surface mixing ratio simply serves as a translation of the CH_4 profile in mixing ratio–altitude space.

We find that a CH_4 surface mixing ratio of 4×10^{-3} and a constant-with-altitude K_{zz} of $1 \times 10^3 \text{ cm}^2 \text{ s}^{-1}$ satisfies the New Horizons data the best. With this K_{zz} profile, the homopause is at Pluto's surface, meaning that molecular diffusion plays an important role throughout Pluto's atmosphere.

3.2. C_2 hydrocarbons

With the CH_4 profile established and a plausible K_{zz} profile defined, we now turn to fitting the profiles of the C_2 hydrocarbons. The New Horizons data show that the concentrations of the C_2 hydrocarbons do not monotonically increase towards the surface of Pluto. Instead, they exhibit inversions between 200 and 400 km, most notably in the cases of C_2H_4 and C_2H_2 . We attribute these inversions to heterogeneous nucleation: in this region of Pluto's atmosphere, the combination of low temperature and high aerosol surface area makes condensation on hydrocarbon/nitrile aerosols the dominant means of removal. The formation and distribution of these aerosols is discussed in Gao et al. (2016). Above 400 km, there are too few nucleation sites for condensation to be important, and below 200 km, the temperature is too high to allow condensation. Compared to the rate of heterogeneous nucleation, the rate of homogeneous nucleation is far too low for it to be a relevant process at these temperatures and concentrations.

A breakdown of the production and loss mechanisms for C_2H_2 , C_2H_4 , and C_2H_6 is presented in Fig. 3. Condensation, shown in black, clearly dominates the region between 200 and 400 km.

Using saturation vapor pressure curves extrapolated to Pluto temperatures results in a condensation-induced inversion of the C_2H_2 profile but not the C_2H_4 profile. Fig. 2b illustrates why: at the relevant temperature of ~ 70 K, the extrapolated saturation vapor pressure of C_2H_4 is several orders of magnitude greater than that of C_2H_2 . Based on the evidence provided at Pluto, we conclude that such an extrapolation of C_2H_4 's saturation vapor pressure is inappropriate and that C_2H_4 should behave similarly to C_2H_2 at low temperatures. Thus, we use C_2H_2 's saturation vapor pressure curve for both C_2H_2 and C_2H_4 , which produces inversions in both species' concentration profiles in our model.

The need to adjust C_2H_4 's extrapolated saturation vapor pressure is not evident from photochemical studies of Titan, where C_2H_4 condenses at temperatures > 80 K (see Fig. 1 of Lavvas et al., 2011), a temperature range for which we have experimental data (Fig. 2a). New Horizons at Pluto probes the hydrocarbon chemistry of a previously unexplored temperature and pressure space.

Early model runs resulted in condensation that was too strong: photochemical production could not compete with condensation, and our concentrations of C_2H_2 and C_2H_4 underestimated the data by up to a factor of 10. We altered the sticking coefficient γ of each individual species to fit their respective abundance profiles. The sticking coefficient is the fraction of collisions that result in a molecule condensing on the surface of an aerosol. We found best-fit sticking coefficients of $\gamma_{\text{C}_2\text{H}_2} = 3 \times 10^{-5}$, $\gamma_{\text{C}_2\text{H}_4} = 1 \times 10^{-4}$, and $\gamma_{\text{C}_2\text{H}_6} = 3 \times 10^{-6}$.

By updating the saturation vapor pressures and introducing variable sticking coefficients, we were able to reproduce the general structure of the C_2 hydrocarbon concentration profiles in Pluto's atmosphere (Fig. 4).

Although the parameters we tuned to fit the CH_4 and C_2 hydrocarbon profiles are related in that they all influence the removal of molecules from the atmosphere, they were tuned in a logical, sequential order. The K_{zz} profile has a far greater influence on CH_4 than it does on the other hydrocarbons due to CH_4 's long chemical lifetime, and since CH_4 is the parent molecule of all photochemical products, it was prudent to adjust the K_{zz} profile to fit the CH_4

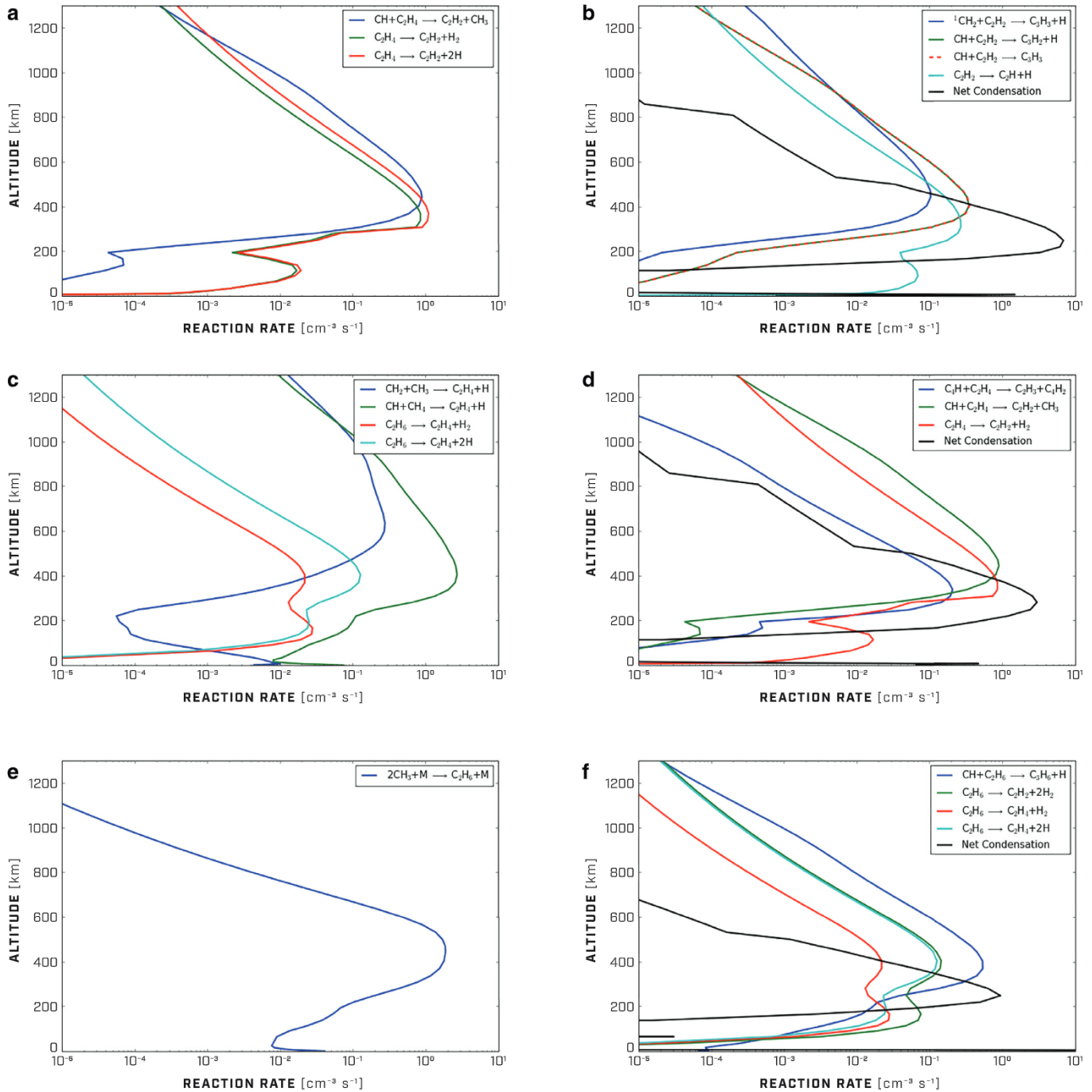


Fig. 3. A breakdown of the mechanisms for production and loss of the major C₂ hydrocarbons at each altitude in Pluto's atmosphere. C₂H₂ production (a) and loss (b). C₂H₄ production (c) and loss (d). C₂H₆ production (e) and loss (f). Between 200 and 400 km, condensation (black) is clearly the dominant loss mechanism for C₂H₂ and C₂H₄, resulting in the inversions in their abundance profiles.

profile first. The concentration profiles of C₂H₂ and C₂H₄ exhibit a condensation-induced inversion between 400 and 200 km; unless C₂H₄'s saturation vapor pressure was lower than its extrapolated value at ~ 70 K, this profile shape could not be achieved. Finally, we tweaked the sticking coefficients of the C₂ species to fit the data more exactly. This systematic tuning reproduced distinct features of Pluto's atmosphere at each step. Varying the K_{zz} profile in a sensible manner, for instance, could not result in the C₂H₄ inversion shape. Similarly, changing the sticking coefficients could not result in the C₂H₄ inversion shape or help with fitting the CH₄ profile.

3.3. HCN

While New Horizons has not provided detailed constraints on the abundance profile of HCN, ALMA data determined an HCN column density of 5×10^{13} molecules cm⁻² (Lellouch et al., 2015). Using an HCN saturation vapor pressure curve extrapolated to Pluto temperatures, we vary the sticking coefficient γ_{HCN} and produce various concentration profiles, each with their own column densities (Fig. 5). We find that $\gamma_{HCN} = 1 \times 10^{-2}$ produces an HCN profile that matches the column density from ALMA observations. That γ_{HCN} is greater than the sticking coefficient of the major C₂

Table 1

The top 10 precipitating species from this work with comparisons, where applicable, to Krasnopolsky and Cruikshank (1999).

Species	Precipitation rate [g cm ⁻² Gyr ⁻¹]	Precipitation rate K&C 1999 [g cm ⁻² Gyr ⁻¹]
C ₂ H ₂	179	195
C ₂ H ₄	95	18
C ₂ H ₆	62	27
CH ₃ C ₂ H	48	
HCN	35	42
C ₆ H ₆	34	
C ₄ H ₂	26	174
C ₃ H ₆	8	
CH ₃ C ₂ CN	6	
HC ₃ N	4	69

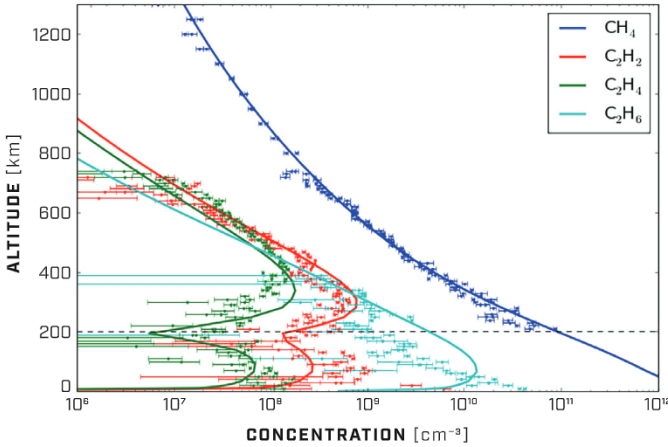


Fig. 4. Best-fit model results for CH₄ and the major C₂ hydrocarbons. The data are from Gladstone et al. 2016, Fig. 2c.

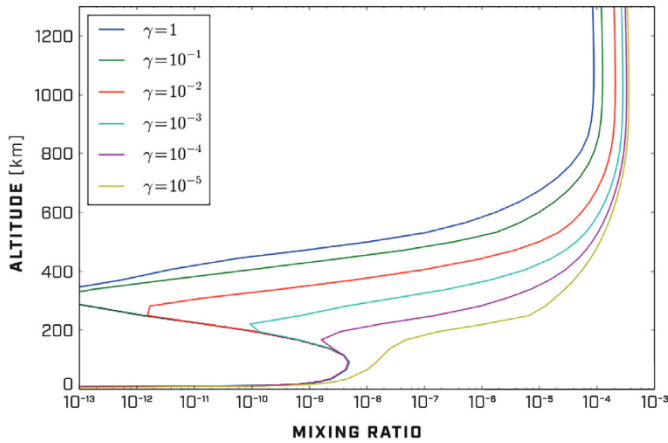


Fig. 5. Various HCN profiles for a range of sticking coefficients γ_{HCN} . The greater the sticking coefficient, the more HCN condenses out of the atmosphere. The HCN column densities range from 1.2×10^{13} ($\gamma_{\text{HCN}} = 1$) to 1.2×10^{15} ($\gamma_{\text{HCN}} = 1 \times 10^{-5}$) molecules cm⁻². A sticking coefficient of $\gamma_{\text{HCN}} = 1 \times 10^{-2}$ gives an HCN column density of 4.8×10^{13} molecules cm⁻², which satisfies the value derived from ALMA observations (Lellouch et al. 2015).

hydrocarbons is consistent with physical intuition: species with larger molecular polarity should be more amenable to sticking.

3.4. Precipitation rates

Krasnopolsky and Cruikshank (1999) report perihelion precipitation rates for C₂H₂, C₄H₂, HC₃N, HCN, C₂H₆, and C₂H₄ of 195, 174, 69, 42, 27, and 18 g cm⁻² Gyr⁻¹, respectively. For those same

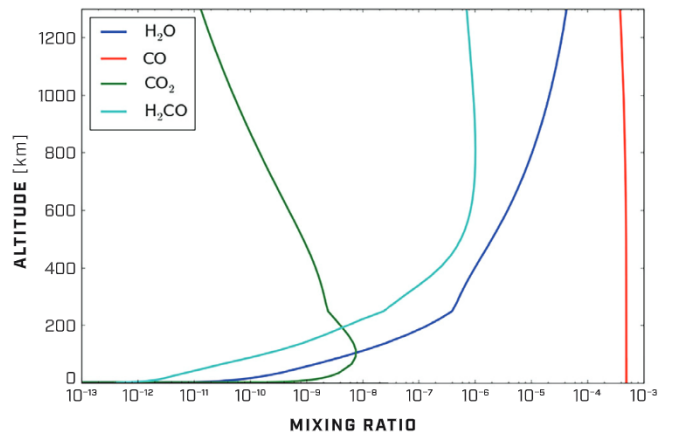


Fig. 6. Model outputs for the major oxygen-bearing species in Pluto's atmosphere.

species, our photochemical model produces precipitation rates of 179, 26, 4, 35, 62, and 95 g cm⁻² Gyr⁻¹. Our precipitation rates for the simpler C₂ hydrocarbons tend to be higher, and we attribute this to our more robust knowledge of their concentration profiles, which showed definite signs of condensation and informed our vapor pressure and sticking coefficient choices. As a consequence of removing the C₂ hydrocarbons faster, our model predicts a lower flux of higher-order hydrocarbons than Krasnopolsky and Cruikshank's (1999) model did. A list of the top 10 precipitating species in our model is presented in Table 1.

3.5. Oxygen chemistry

Despite there being very few observational constraints for oxygen-bearing species in Pluto's atmosphere, they must certainly be present, as carbon monoxide is the third most abundant gas. In our model, we set the surface mixing ratio of CO to 5×10^{-4} (Lellouch et al., 2011), and include an exogenous H₂O flux of $\sim 5 \times 10^5$ molecules cm⁻² s⁻¹ at the top of the atmosphere (Poppe, 2015). With these boundary conditions, our photochemical model predicts abundance profiles for oxygen-bearing molecules (Fig. 6) which may later be verified by future observations and data analysis.

4. Conclusions

Although the atmospheres of Pluto and Titan share the same cast of characters—N₂, CH₄, CO, and their photochemical derivatives—the stories that they tell are different. Through linking specific unique outcomes with specific unique situational parameters, we can illuminate new knowledge about the physics and chemistry of planetary atmospheres. Each new planetary body that

we visit is a brand new experiment that Nature has performed for our eyes to see and our minds to ponder. Pluto, the most distant object that humankind's mechanical proxies have encountered to date, represents Nature's laboratory for organic photochemistry at extremely low pressures and temperatures.

By fitting New Horizons' CH₄ profile, we gained knowledge about Pluto's eddy diffusion profile and surface CH₄ mixing ratio. By fitting New Horizons' C₂ hydrocarbon profiles, we learned about the saturation vapor pressures of C₂ hydrocarbons and their sticking coefficients at temperatures that have never been probed before. By fitting the HCN column density from ALMA observations, we have suggested a sticking coefficient for HCN as well. Finally, we make predictions for the abundances of oxygen-bearing species in Pluto's atmosphere. The proposed vapor pressure changes and the sticking coefficients could be tested by appropriate experiments in the laboratory, and future missions and observations can reveal Pluto's oxygen chemistry and validate or otherwise the results of this model.

Acknowledgments

This research was supported in part by a grant from the New Horizons mission. YLY and RLS were supported in part by the Cassini UVIS program via NASA Grant JPL1459109, NASA NNX09AB72G grant to the California Institute of Technology. PG was supported in part by an RTD grant from JPL. MLW is grateful to Theater Arts at Caltech as a source of personal motivation by giving him the chance to portray Clyde Tombaugh in *Planet Between the Stars* during the course of this project.

References

- Allen, M., Yung, Y.L., Waters, J.W., 1981. Vertical transport and photochemistry in the terrestrial mesosphere and lower thermosphere (50–120 km). *J. Geophys. Res.* 86, 3617–3627. doi:[10.1029/JA086iA05p03617](https://doi.org/10.1029/JA086iA05p03617).
- Gao, P., Fan, S., Wong, M.L., Liang, M.-C., Shia, R.-L., Kammer, J.A., Summers, M.E., Gladstone, G.R., Young, L.A., Olkin, C.B., Ennico, K., Weaver, H.A., Stern, S.A., Yung, Y.L., New Horizons Science Team, 2016. Microphysics of Pluto's photochemical haze and comparison to new horizons observations. *Icarus*.
- Gladstone, G.R., Pryor, W.R., Alan Stern, S., 2015. Ly α @Pluto. *Icarus* 246, 279–284. doi:[10.1016/j.icarus.2014.04.016](https://doi.org/10.1016/j.icarus.2014.04.016).
- Gladstone, G.R., Stern, S.A., Ennico, K., Olkin, C.B., Weaver, H.A., Young, L.A., Summers, M.E., Strobel, D.F., Hinson, D.P., Kammer, J.A., Parker, A.H., Steffl, A.J., Lin-scott, I.R., Parker, J.W., Cheng, A.F., Slater, D.C., Versteeg, M.H., Greathouse, T.K., Rutherford, K.D., Throop, H., Cunningham, N.J., Woods, W.W., Singer, K.N., Tsang, C.C.C., Schindhelm, E., Lisse, C.M., Wong, M.L., Yung, Y.L., Zhu, X., Curdt, W., Lavvas, P., Young, E.F., Tyler, G.L., 2016. The atmosphere of Pluto as observed by New Horizons. *Science* 351, 1280. doi:[10.1126/science.aad8866](https://doi.org/10.1126/science.aad8866).
- Krasnopolsky, V.A., Cruikshank, D.P., 1999. Photochemistry of Pluto's atmosphere and ionosphere near perihelion. *J. Geophys. Res.* 104, 21979–21996.
- Lara, L.M., Lellouch, E., López-Moreno, J.J., Rodrigo, R., 1996. Vertical distribution of Titan's atmospheric neutral constituents. *J. Geophys. Res.* 101, 23261. doi:[10.1029/96JE02036](https://doi.org/10.1029/96JE02036).
- Lavvas, P., Griffith, C.A., Yelle, R.V., 2011. Condensation in Titan's atmosphere at the Huygens landing site. *Icarus* 215, 732–750. doi:[10.1016/j.icarus.2011.06.040](https://doi.org/10.1016/j.icarus.2011.06.040).
- Lellouch, E., de Bergh, C., Sicardy, B., Käufl, H.U., Smette, A., 2011. High resolution spectroscopy of Pluto's atmosphere: detection of the 2.3 μm CH₄ bands and evidence for carbon monoxide. *Astron. Astrophys.* 530, L4.
- Lellouch, E., Gurwell, M., Butler, B., Moullet, A., Moreno, R., Bockelée-Morvan, D., Biver, N., Fouchet, T., Lis, D., Stern, A., Young, L., Young, E., Weaver, H., Boissier, J., Stansberry, J., 2015. Detection of HCN in Pluto's atmosphere. *American Astronomical Society, DPS Meeting #47*, id.105.07.
- Li, C., Zhang, X., Gao, P., Yung, Y., 2015. Vertical distribution of C3-Hydrocarbons in the stratosphere of Titan. *Astrophys. J. Lett.* 803, L19. doi:[10.1088/2041-8205/803/2/L19](https://doi.org/10.1088/2041-8205/803/2/L19).
- Moses, J.I., Allen, M., Yung, Y.L., 1992. Nucleation and aerosol formation Neptune's atmosphere. *Icarus* 99, 318–346.
- Poppe, A.R., 2015. Interplanetary dust influx to the Pluto – Charon system. *Icarus* 246, 352–359. doi:[10.1016/j.icarus.2013.12.029](https://doi.org/10.1016/j.icarus.2013.12.029).
- Willacy, K., Allen, M., Yung, Y.L., 2016. A new astrobiological model of the atmosphere of Titan. *Astrophys. J.* 829. doi:[10.3847/0004-637X/829/2/79](https://doi.org/10.3847/0004-637X/829/2/79).
- Wong, M.L., Yung, Y.L., Gladstone, G.R., 2015. Pluto's implications for a snowball Titan. *Icarus* 246, 192–196. doi:[10.1016/j.icarus.2014.05.019](https://doi.org/10.1016/j.icarus.2014.05.019).
- Yung, Y.L., Allen, M., Pinto, J.P., 1984. Photochemistry of the atmosphere of Titan: comparison between model and observations. *Astrophys. J. Suppl. Ser.* 55, 465–506.
- Yung, Y.L., DeMore, W.B., 1999. *Photochemistry of Planetary Atmospheres*. Oxford.